

Experimental estimation of the electric dipole moment and polarizability of titanyl phthalocyanine using ultraviolet photoelectron spectroscopy

H. Fukagawa,^{1,2} H. Yamane,¹ S. Kera,^{1,2} K. K. Okudaira,^{1,2} and N. Ueno^{1,2}

¹Faculty of Engineering, Chiba University, Inage-ku, Chiba 263-8522, Japan

²Graduate School of Science and Technology, Chiba University, Yayoi-cho, Inage-ku, Chiba 263-8522, Japan

(Received 22 August 2005; revised manuscript received 6 December 2005; published 4 January 2006)

Changes in the work function (WF) and binding energy of the highest occupied molecular orbital (HOMO) level in a titanyl phthalocyanine (OTiPc) graphite system were studied as a function of OTiPc coverage by ultraviolet photoelectron spectroscopy. We observed that the WF increases with the coverage of the oriented OTiPc until the formation of the monolayer, while the energy position of the HOMO level stays almost unchanged with respect to the Fermi level. By analyzing the observed coverage dependence of the WF using the Topping model, we estimated the electric dipole moment and polarizability of OTiPc in a monolayer.

DOI: [10.1103/PhysRevB.73.041302](https://doi.org/10.1103/PhysRevB.73.041302)

PACS number(s): 73.30.+y, 73.20.-r, 79.60.Dp

Organic optoelectronic devices have attracted attention in recent years due to their various applications and flexibility.¹ An electric dipole layer at an organic and/or metal interface participates in the collection and injection of charges at the interface and plays an important role in the performance of the devices.² Campbell and co-workers,³ and Ganzorig *et al.*⁴ demonstrated that a Schottky barrier can be manipulated by the insertion of a dipole layer between a metal and an organic material, using self-assembled monolayers (SAMs) with a chemical moiety of an electric dipole. However, it is not clear whether a thermodynamic equilibrium is achieved in these systems because of the strong insulating nature of the alkyl chains in SAMs. Recently, Kera *et al.*⁵ have demonstrated quantitatively that an interface dipole layer induces a change in the binding energy of the highest occupied molecular orbital (HOMO) level, which is equal to a change in work function (WF) for a well-defined system in which a thermodynamic equilibrium is achieved. The molecular electric dipole, interfacial electric dipole, and interfacial polarizability are directly associated with the carrier dynamics at organic and/or metal interfaces.⁶ However, the lack of the experimental values of the electric dipole moment and polarizability of a molecule has hindered quantitative studies on the energy level alignment and energetics of carriers at the interfaces. As a result, the effects of molecular dipoles on these issues have been discussed using theoretical values.³ For more quantitative studies, it is thus necessary to obtain the experimental values of the electric dipole moment and polarizability of the molecule used in an organic device.

In general, the adsorption of molecules onto a solid surface causes changes in their charge distributions near the surface, leading to the creation of a surface dipole layer. As a consequence, the modifications of the WF are observed.⁷ In the past, the WF change related to interface dipole in SAMs has been successfully analyzed using Helmholtz equation that is derived for a continuous dipole sheet.⁸⁻¹⁰ In these analyses, however, the effect of the dipole-dipole interaction, which causes a depolarization field at a certain position of the molecule depending on the arrangement of all surrounding molecular dipoles, is not positively considered. On the other hand, Topping proposed a depolarization model based

on the calculations for a planar sheet of evenly spaced dipoles on either a square or hexagonal lattice.¹¹ In this model, the electric dipole moment and polarizability of a surface-molecule complex can be determined from the coverage dependence of the WF in the limit of zero coverage.¹² This model is an alternative to the analysis method using Helmholtz equation and has been widely used in analyzing the change in WF by many groups mainly for inorganic systems.¹²⁻¹⁵ The reason why this model has not been applied to organic systems is that it is difficult to control the surface coverage of large molecules in organic dipole layer systems such as SAMs. In this paper, we applied this model to the analysis of the change in the WF of a well-defined dipole layer system, which consists of a π -conjugated molecule with an electric dipole moment and an inert substrate surface, to estimate experimentally the electric dipole moment and polarizability of the molecule.

Ultraviolet photoelectron spectroscopy (UPS) measurements were performed for thin films of titanyl phthalocyanine (OTiPc), which has an electric dipole moment perpendicular to the molecular plane, vacuum deposited on graphite. On graphite, the molecule-substrate interaction is very small due to a weak van der Waals interaction, and thus an intentional dipole layer can be realized by preparing an oriented OTiPc layer.^{5,16} We studied the WF change in the OTiPc/graphite system as a function of the coverage of the molecule by UPS, and observed a continuous increase in WF during monolayer formation. By analyzing the observed WF shift using the Topping model, we estimated the electric dipole moment and polarizability of the OTiPc molecule in the monolayer for the first time.

HeI UPS spectra were measured using the previously described apparatus.¹⁷ The total instrumental energy resolution of the present measurements was less than 60 meV as measured from the Fermi edge of an evaporated Au film. The sample was biased by -5.0 V so that the secondary-electron cutoff of the spectrum would yield the vacuum level (VL). The energy difference between the VL and the Fermi level corresponds to the WF of the sample. A highly oriented pyrolytic graphite (HOPG)/ZYA-grade substrate was cleaved in air immediately before loading into a sample-preparation

chamber ($\sim 10^{-8}$ Pa), and typically cleaned by *in situ* heating at 620 K for 15 h. The purified OTiPc was carefully evaporated onto the HOPG substrate in the sample-preparation chamber at a substrate temperature of 295 K. The amount and rate (0.05 nm/min) of deposition were measured with a quartz microbalance. The sample was then introduced into the measurement chamber for *in situ* measurements. We repeatedly conducted deposition, sample annealing, and UPS measurement. All UPS spectra were measured at 295 K after annealing the films at 420 K for 3 h.

Prior to showing the experimental results, we briefly summarize the previous results of the growth of OTiPc thin films on HOPG, namely, the change in molecular orientation with increasing film thickness and the effect of annealing on the molecular orientation.^{18,19} In the as-grown OTiPc film on HOPG with a monolayer and a submonolayer of nominal thickness, molecules form bilayer islands in which most of the molecules in the outer layer are oriented flat with the oxygen atom directed inward to the substrate (*downward orientation*). Upon annealing at 373–423 K for 3–12 h, the molecules spread from the islands over the substrate surface to form monolayer domains in which all the molecules are oriented flat with the oxygen atom directed outward to the vacuum (*upward orientation*). When the second layer of OTiPc is deposited on this monolayer, the molecules in the outer layer exhibit a *downward orientation*. In the oriented monolayer, the electric dipole moments of the molecules are parallel and form a dipole layer, while in the bilayer, the electric dipole moments of the first and second layers cancel each other. These changes in molecular orientation were detected by metastable-atom electron spectroscopy,²⁰ and the corresponding WF shift was observed by UPS.²¹

Examples of HeI UPS spectra of OTiPc on HOPG are shown as a function of deposition amount (δ) in Figs. 1(a) and 1(b), for the VL and HOMO band regions, respectively. The binding energy (E_B) was measured from the Fermi level of the substrate (E_F^{sub}). The angle between the incident photons and the emitted electrons was fixed to be 45° . The spectra of the VL region were measured at an electron takeoff angle of 0° (normal emission) and a photon incidence angle of 45° . The spectra of the HOMO band region were measured at an electron takeoff angle of 45° and a photon incidence angle of 0° (normal incidence). As seen in Fig. 1(a), the VL first increases for $0 \leq \delta \leq 0.38$ nm with δ , then decreases for $0.38 \leq \delta \leq 1.28$ nm and remains constant for $1.28 \text{ nm} \leq \delta$. In Fig. 1(b), on the other hand, the HOMO band shows small changes in position and shape for $0 \leq \delta \leq 0.38$ nm, and broadens with δ until $\delta = 0.88$ nm. Finally, the intensity of the higher E_B side component increases for $1.08 \leq \delta$. These δ dependences of the VL and HOMO band position are not parallel, which is different from that observed conventional organic and/or metal systems.⁷ To clarify this phenomenon, we mapped the intensities of the HeI UPS spectra for the VL and HOMO band regions as a function of δ in Fig. 2, where the results not shown in Fig. 1 are included. In Fig. 2, the horizontal axis represents δ (nanometers) and the vertical axis represents the electron energy relative to E_F^{sub} . To map the UPS spectra intensities, the background photoelectrons from the substrate was subtracted

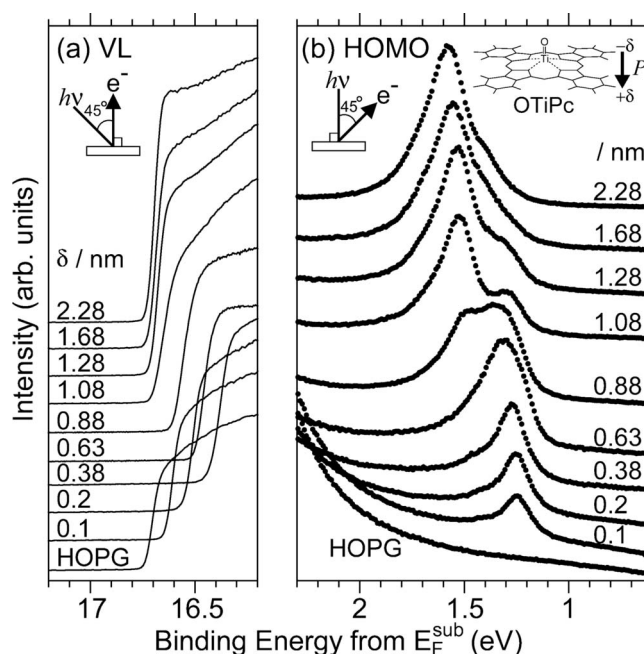


FIG. 1. Examples of HeI UPS spectra as a function of deposition amount of OTiPc (δ) on HOPG in VL region (a) and HOMO band region (b). All of the spectra are measured at 295 K after annealing each film at 420 K for 3 h with a -5 V bias applied to the sample to observe the VL. The E_B scale refers to E_F^{sub} . The angle between the incident photons and the emitted electron is fixed to be 45° . The spectra of the VL region are measured at a photoelectron takeoff angle of 0° (normal emission) and the spectra of the HOMO band region are measured at a photoelectron takeoff angle of 45° (normal incidence). The inset illustration shows the schematics of the direction of the molecular electric dipole moment (P) and optimized molecular structure of OTiPc from MO calculation.

for the HOMO band region. The secondary electron cutoff corresponds to the VL as shown in Fig. 2 (white dotted line). The schematic of the expected molecular orientation at each δ is also shown.^{18,19} It is clearly seen that the WF increases continuously with increasing δ up to $\delta = 0.38$ nm at about 0.29 eV and then decreased, reaching a constant value, which is similar to that of HOPG, at about $\delta \sim 1.28$ nm. By considering the molecular orientation and the electrostatic potential due to permanent dipole of OTiPc (dipole potential),¹⁸ these results indicate that (i) the monolayer of OTiPc is formed at $\delta \sim 0.38$ nm [point (A) in Fig. 2] and (ii) the bilayer formation starts at $\delta = 0.38$ nm [region (II) in Fig. 2] and stops at $\delta \sim 1.28$ nm [point (B) in Fig. 2], where the dipoles in the first layer are canceled by those in the second layer. The bilayer formation at about $\delta \sim 1.28$ nm can be confirmed by the increase in the E_B position of the HOMO (point B), where the dipole layer due to the oriented monolayer is completely cancelled by that of the second layer.²¹ In this paper, we note the change in the electronic structure in monolayer formation region (I), although those in regions (II) and (III) are also of interest.

The observed continuous WF change during monolayer formation is caused by the change in averaged dipole potential that depends on the coverage of *upward* OTiPc. It is worth noting, on the other hand, that the E_B position of the

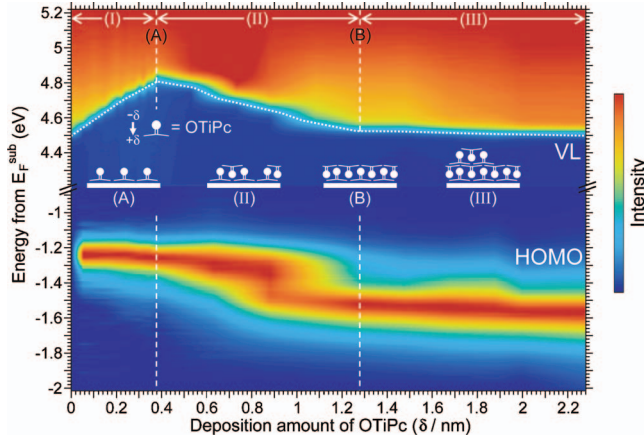


FIG. 2. (Color) Map of HeI UPS spectra intensities for VL and HOMO band regions of OTiPc/HOPG system as a function of deposition amount (δ). The vertical axis represents the electron energy relative to E_F^{sub} . The VL corresponds to the cutoff of the secondary electron (indicated by the white dotted line). (I)–(III) indicate the regions of the monolayer and double layer formation, and (A) or (B) corresponds to δ of the monolayer and double layer being formed. The schematic of expected molecular orientation at each deposition amount is also shown.

HOMO relative to E_F^{sub} slightly changes during monolayer formation. We indicate that the change in WF reflects the dipole potential of the system averaged over a wider area, while the E_B position of the HOMO relative to E_F^{sub} is affected by the dipole potential that acts on each molecule.¹⁷ Evidence that the E_B position of the HOMO relative to E_F^{sub} is not determined by the averaged dipole potential can be seen not only in region (I) but also in region (II) in Fig. 2, where the E_B position of the HOMO stay unchanged while WF decreases drastically depending on the coverage of downward OTiPc. We can obtain the electric dipole moment (P) and polarizability (α) of OTiPc by analyzing of the present WF data for the OTiPc/HOPG system during monolayer formation within the Topping model. For a semiconductor, a change in WF results from two contributions:¹³ (i) the contribution of the dipole layer $e\Delta\phi_{\text{Dip}}$ and (ii) the adsorbate-induced change in surface potential due to charge exchange through the interface (band bending) $e\Delta V_s$. The total WF change $e\Delta\phi$ is therefore given by

$$e\Delta\phi = e\Delta\phi_{\text{Dip}} + e\Delta V_s. \quad (1)$$

In the OTiPc/HOPG system, we can assume $e\Delta V_s = 0$ since the interaction and charge exchange between the molecule and the HOPG substrate are very small (~ 10 meV) compared with $e\Delta\phi$ observed in the present experiments.^{5,16,22} The observed WF change is thus dominated by the oriented permanent dipole density of OTiPc. In this case, $e\Delta\phi_{\text{Dip}}$ is expressed as¹⁴

$$e\Delta\phi_{\text{Dip}} = \pm \frac{e}{\epsilon_0} P n_{\text{Dip}} \left(1 + \frac{9\alpha}{4\pi} n_{\text{Dip}}^{3/2} \right)^{-1}, \quad f_{\text{dep}} = \frac{9\alpha}{4\pi} n_{\text{Dip}}^{3/2}, \quad (2)$$

where n_{Dip} and ϵ_0 are the dipole density and vacuum permittivity, respectively. The dipole density may be expressed as¹⁵

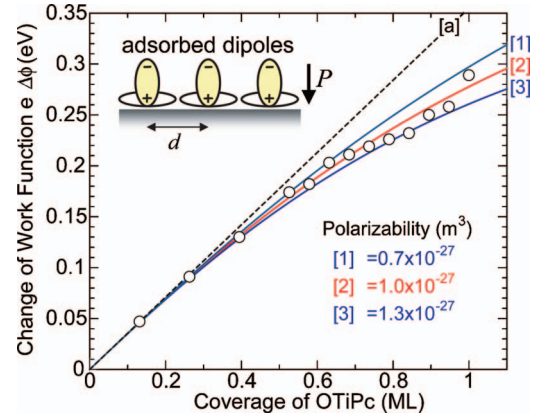


FIG. 3. (Color) Dependence of sample work function (WF) on OTiPc coverage, where 1 ML corresponds to $\delta = 0.38$ nm (see Fig. 2). In the low coverage region (~ 0.3 ML), the WF changes along the dashed line (a). The colored curves represent fitting curves with different polarizabilities determined using the Topping model. The schematic representation of the molecular orientation and the direction of the dipole (P) in the monolayer of OTiPc are also shown.

$$n_{\text{Dip}} = \frac{\theta}{d^2} b, \quad (3)$$

where θ is the coverage of OTiPc ($0 \leq \theta \leq 1$), d is the lattice constant of this system, and b is a constant related to the lattice structure of adsorbed molecules. The second term in parentheses in Eq. (2), called the depolarization factor f_{dep} , is a correction to the WF change due to the interaction between the dipoles, which reduces the effective electric field at the site of a particular dipole. Here, we assume that the lattice constant of the present monolayer is the same as that of a CuPc/HOPG system with a square unit cell of 1.37 nm \times 1.37 nm.²³ For a square surface unit cell, $b = 1$.¹⁵

Figure 3 shows the WF vs OTiPc coverage (O) plot and some fitting curves, where 1 monolayer (ML) corresponds to $\delta = 0.38$ nm. A clear WF change of about 0.29 eV is observed after the deposition of 1 ML of OTiPc. First, we obtain P by analyzing the δ dependence of the VL, which directly corresponds to the δ dependence of the WF, in the low coverage region. For the low coverage region ($n_{\text{Dip}} \ll 1$), we obtain the following relation, since $f_{\text{dep}} \ll 1$.

$$e\Delta\phi = \pm \frac{e}{\epsilon_0} P n_{\text{Dip}}. \quad (4)$$

In this case, the WF increases linearly with n_{Dip} and thus P is determined by the slope of the $e\Delta\phi$ vs n_{Dip} plot. Thus, the initial variation in WF for the low OTiPc coverage region gives P . In the low OTiPc coverage region (~ 0.3 ML), we see that the WF changes nearly linearly with δ , as shown by the dashed line (a) in Fig. 3. We obtained $P \cong 1.77 \pm 0.05$ D from the slope of the dashed line (a). The present experimental value is smaller than the calculated value (3.73 D) using the density functional theory (DFT) method with B3LYP/LanL2DZ in the optimized structure. We performed some other calculations of P and found that the calculated value is very sensitive to the distance between O and Ti. We speculate that the difference between the experimental and calculated P values originates mainly from the difference in

chemical structure between free and adsorbed molecules. The Topping model is applicable to the system where molecules do not aggregate to form an island but distribute uniformly on the surface even below monolayer region.¹¹ The fact that the WF changes nearly linearly with δ and the additional step structure in the cutoff region of secondary electrons is not observed in Fig. 1; (a) demonstrates that the molecules do not form large islands on the surface, although the details of the film growth model have not yet been clarified. If the molecules came together in a large domain, a large potential difference would appear between the molecule-covered region and the bare region of the substrate, resulting in the formation of an additional structure in the cutoff region.²¹

Using the obtained P value, we analyzed the WF change in the high coverage region using Eq. (2) by setting the polarizability as a variable parameter [colored lines (1)–(3) in Fig. 3], and determined the polarizability of OTiPc to be $\alpha \cong (1.0 \pm 0.3) \times 10^{-27} \text{ m}^3$. In passing, we estimated the dielectric constant of the OTiPc monolayer system from the Helmholtz equation.⁹ The potential change ΔV is described by the Helmholtz equation,

$$\Delta V = \frac{\mu \cos \varphi}{\epsilon \epsilon_0}, \quad (5)$$

where μ is the dipole moment per area, φ is the angle between dipole and surface normal.⁹ The density of dipoles is

assumed to be $1/1.37 \times 1.37 \text{ nm}^2$. Using the obtained P and observed WF change, we determined ϵ to be about 1.22. The dielectric constant of large molecules estimated in molecular sheet of flat-lie system is smaller than other organic dipole layer system such as SAMs because the dipole density is small.⁹

In conclusion, we observed a continuous WF change with the coverage of a polarized molecule on an inert graphite substrate surface. The observed WF change is dominated by the effect of the change in the coverage of the polarized molecule. By analyzing the present WF change using the Topping model, we obtained the electric dipole moment and polarizability of OTiPc in a monolayer. In addition, we estimated the dielectric constant of the OTiPc in a monolayer, and found that the estimated value is smaller than other organic dipole layer system such as SAMs because the dipole density is small.

This work was partly supported by the NEDO International Joint Research Grant Program (Grant No. 2002BR030), Grant-in-Aid for Creative Scientific Research of JSPS (Grant No. 14GS0213), Grand-in-Aid for Young Scientists (A), JSPS for Young Scientist, and 21st Century COE Program (establishment of COE of organic device physics).

-
- ¹W. R. Salaneck, K. Seki, A. Kahn, and J. J. Pireaux, *Conjugated Polymer and Molecular Interfaces* (Marcel Dekker, New York, 2002).
- ²D. Cahen, A. Kahn, and E. Umbach, *Mater. Today* **8**, 32 (2005).
- ³I. H. Campbell, J. D. Kress, R. L. Martin, D. L. Smith, N. N. Barashkov, and J. P. Ferraris, *Appl. Phys. Lett.* **71**, 3528 (1997).
- ⁴C. Ganzorig, K.-J. Kwak, K. Yagi, and M. Fujihira, *Appl. Phys. Lett.* **79**, 272 (2001).
- ⁵S. Kera, Y. Yabuuchi, H. Yamane, H. Setoyama, K. K. Okudaira, A. Kahn, and N. Ueno, *Phys. Rev. B* **70**, 085304 (2004).
- ⁶V. S. L'vov, R. Naaman, V. Tiberkevich, and Z. Vager, *Chem. Phys. Lett.* **381**, 650 (2003).
- ⁷H. Ishii, K. Sugiyama, E. Ito, and K. Seki, *Adv. Mater. (Weinheim, Ger.)* **11**, 605 (1999).
- ⁸S. D. Evans, E. Urankar, A. Ulman, and N. Ferris, *J. Am. Chem. Soc.* **113**, 4121 (1991).
- ⁹M. Bruening, R. Cohen, J. F. Guillemoles, T. Moav, J. Libman, A. Shanzer, and D. Cahen, *J. Am. Chem. Soc.* **119**, 5720 (1997).
- ¹⁰G. Ashkenasy, D. Cahen, R. Cohen, A. Shanzer, and A. Vilan, *Acc. Chem. Res.* **35**, 121 (2002).
- ¹¹J. Topping, *Proc. R. Soc. London, Ser. A* **114**, 67 (1927).
- ¹²R. W. Verhoef and M. Asscher, *Surf. Sci.* **391**, 11 (1997).
- ¹³H. Lüth, *Surface and Interfaces of Solid Materials* (Springer-Verlag, Berlin, 1995), p. 509.
- ¹⁴G. Gensterblum, K. Hevesi, B.-Y. Han, L.-M. Yu, J.-J. Pireaux, P. A. Thiry, R. Caudano, A.-A. Lucas, D. Bernaerts, S. Amelinckx, G. Van Tendeloo, G. Bendele, T. Buslaps, R. L. Johnson, M. Foss, R. Feidenhans'l, and G. Le Lay, *Phys. Rev. B* **50**, 11981 (1994), and references therein.
- ¹⁵M. Pivetta, F. Patthey, W.-D. Schneider, and B. Delley, *Phys. Rev. B* **65**, 045417 (2002), and references therein.
- ¹⁶S. Kera, H. Yamane, I. Sakuragi, K. K. Okudaira, and N. Ueno, *Chem. Phys. Lett.* **364**, 93 (2002).
- ¹⁷H. Fukagawa, H. Yamane, S. Kera, K. K. Okudaira, and N. Ueno, *IPAP Conf. Ser.* **6**, 73 (2005).
- ¹⁸S. Kera, K. K. Okudaira, Y. Harada, and N. Ueno, *Jpn. J. Appl. Phys., Part 1* **40**, 783 (2001).
- ¹⁹S. Kera, A. Abduaini, M. Aoki, K. K. Okudaira, N. Ueno, Y. Harada, Y. Shiota, and T. Tsuzuki, *Thin Solid Films* **327–329**, 278 (1998).
- ²⁰Y. Harada, S. Masuda, and H. Ozaki, *Chem. Rev. (Washington, D.C.)* **97**, 1897 (1997).
- ²¹H. Yamane, H. Honda, H. Fukagawa, M. Ohyama, Y. Hinuma, S. Kera, K. K. Okudaira, and N. Ueno, *J. Electron Spectrosc. Relat. Phenom.* **137–140**, 223 (2004).
- ²²H. Yamane, Y. Yabuuchi, H. Fukagawa, S. Kera, K. K. Okudaira, and N. Ueno (unpublished).
- ²³C. Ludwig, R. Strohmaier, J. Petersen, B. Gompf, and W. Eisenmenger, *J. Vac. Sci. Technol. B* **12**, 1963 (1994).